SECTION 2
MECHANICAL PROPERTIES OF FLUID DAMPERS

2.1 Description of Dampers

Damping devices which utilize fluid flow through orifices were originally developed for the shock isolation of military hardware. To appreciate the level of technology involved in these shock isolation systems, note that the so-called weapons grade shock usually has free field input wave forms with peak velocities in excess of 180 in/sec (4572 mm/sec), rise times of less than 2 msecs and peak accelerations of the order of 200g (Clements 1972).

The fluid dampers under investigation evolved from these shock isolation damping devices. The construction of the tested device is shown in Figure 2-1. It consists of a stainless steel piston, with a bronze orifice head and an accumulator. It is filled with silicone oil. The orifice flow is compensated by a passive bi-metallic thermostat that allows operation of the device over a temperature range of -40°F to 160°F (-40°C to 70°C). The orifice configuration, mechanical construction, fluid and thermostat used in this device originated within a device used in a classified application on the U.S. Air Force B-2 Stealth Bomber. Thus, the device includes performance characteristics considered as state of the art in hydraulic technology.

2.2 Operation of Dampers

The force that is generated by the fluid damper is due to a pressure differential across the piston head. Consider that the piston moves from left to right in Figure 2-1 (device subjected to compression force). Fluid flows from chamber 2 towards chamber 1. Accordingly, the damping force is proportional to the pressure differential in these two chambers. However, the fluid volume is reduced by the product of travel and piston rod area. Since the

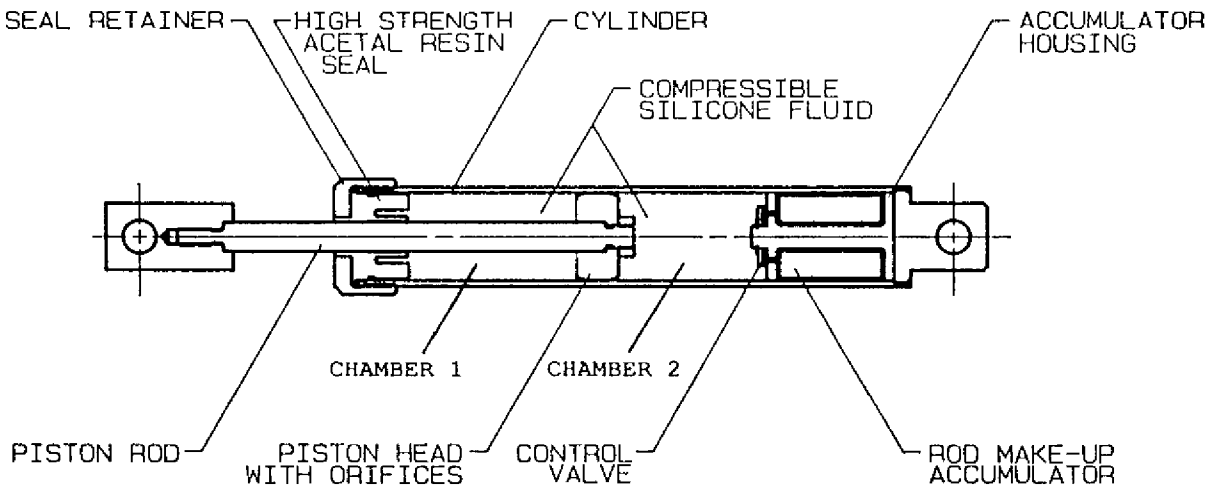

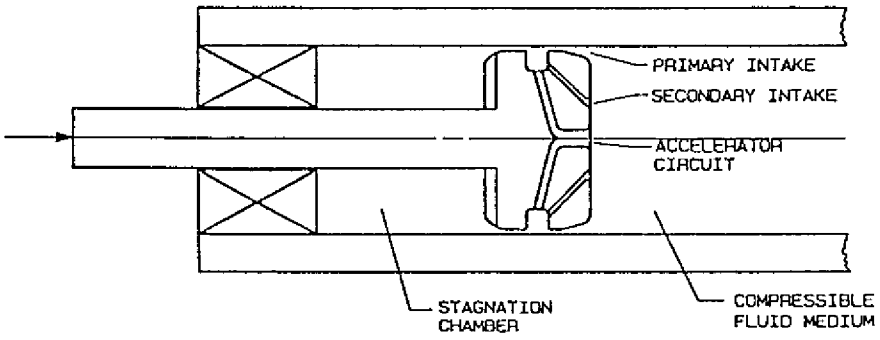

Fluidic Control Orifice

FIGURE 2-1 Construction of Fluid Viscous Damper

fluid is compressible, this reduction in fluid volume is accompanied by the development of a restoring (spring like) force. This is prevented by the use of the accumulator. The tested device showed no measurable stiffness for piston motions with frequency less than about 4 Hz. In general, this cutoff frequency depends on the design of the accumulator and may be specified in the design.

The existence of the aforementioned cutoff frequency is a desirable property. The devices may provide additional viscous type damping to the fundamental mode of the structure (typically with a frequency less than the cutoff frequency) and additional damping and stiffness to the higher modes. This may, in effect, completely suppress the contribution of the higher modes of vibration.

The force in the fluid damper may be expressed as

$$P = bp_{12} \tag{2-1}$$

where p_{12} is the pressure differential in chambers 1 and 2. Constant b is a function of the piston head area, A_p, piston rod area, A_r, area of orifice, A_1, number of orifices, n, area of control valves, A_2 and the discharge coefficient of the orifice, C_{d1} and control valve, C_{d2}.

The pressure differential across the piston for cylindrical orifices is given by

$$p_{12} = \frac{\rho}{2n^2 C_{d1}^2}\left(\frac{A_p}{A_1}\right)^2 \dot{u}^2 \, sgn\,(\dot{u}) \tag{2-2}$$

where ρ is the fluid density and $\dot{u}$ is the velocity of the piston with respect to the housing.

In cylindrically-shaped orifices, the pressure differential is proportional to the piston velocity squared. Such orifices are

termed "square law" or "Bernoullian" orifices since Equation 2-2 is predicted by Bernoulli's equation. Bernoullian orifices produce damper forces which are proportional to velocity squared, a usually unacceptable performance in shock isolation.

The orifice design in the tested fluid damper produces a force that is not proportional to velocity squared. The orifice utilizes a series of specially shaped passages to alter flow characteristics with fluid speed. A schematic of this orifice is shown in Figure 2-1. It is known as Fluidic Control Orifice. It provides forces which are proportional to $|\dot{u}|^{\alpha}$, where α is a predetermined coefficient in the range of 0.5 to 1.2. A design with coefficient α equal to 0.5 is useful in applications involving extremely high velocity shocks. They are typically used in the shock isolation of military hardware. In applications of earthquake engineering, a design with $\alpha = 1$ appears to be the most desired one. It results in essentially linear viscous behavior. The devices utilized in this testing program were designed to have this behavior.

2.3 Testing Arrangement and Procedure

The mechanical characteristics of the dampers have been determined using the testing arrangement shown in Figures 2-2 and 2-3. A hydraulic actuator applies a dynamic force along the axis of the damper. The force in the damper is measured using a load cell which is connected between the damper and the reaction frame. The displacement of the damper is measured using an LVDT (Linear Variable Differential Transformer) which is located within the actuator. The force-displacement relationship can now be obtained and used to extract the mechanical characteristics of the dampers.

Figure 2-4 and Table 2-I show dimensional and other characteristics of the tested damper and other commercially available dampers. It

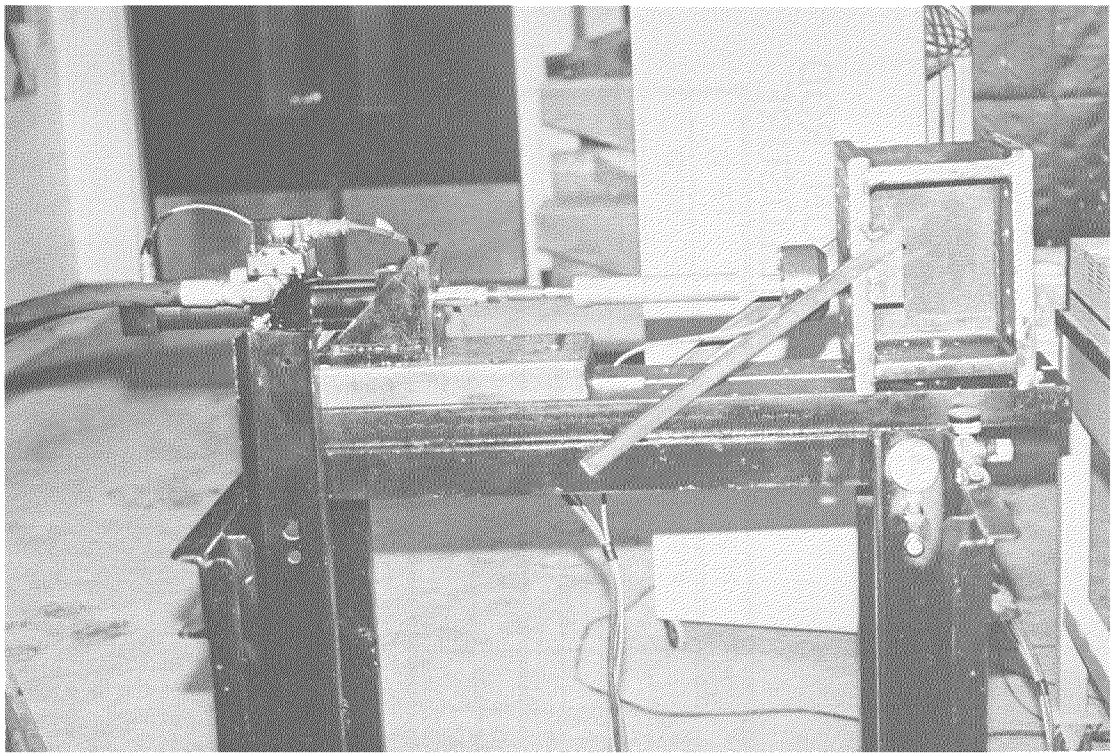

FIGURE 2-2 View of Testing Arrangement

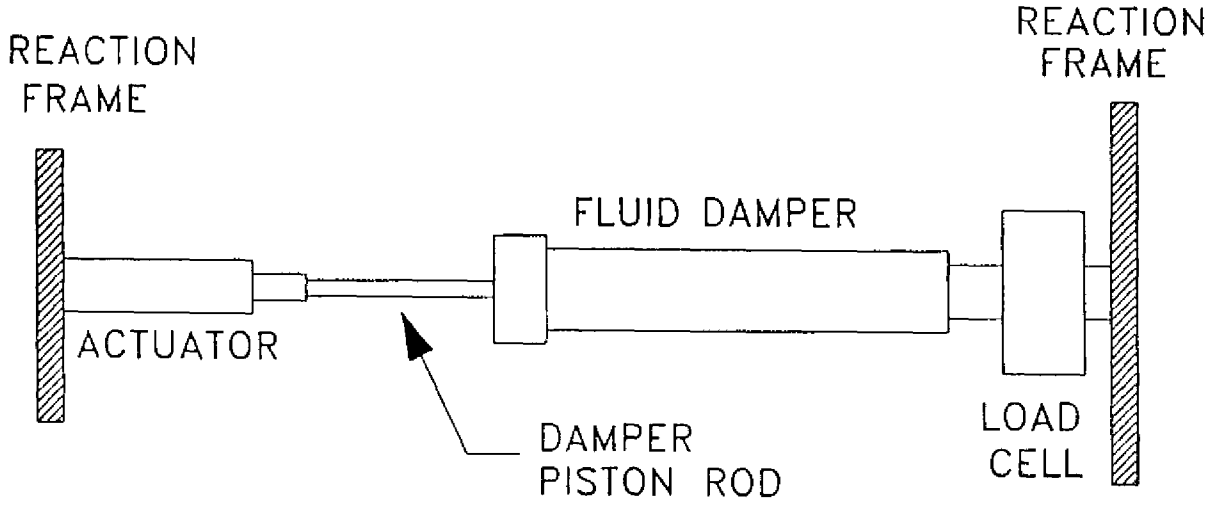

FIGURE 2-3 Schematic of Testing Arrangement

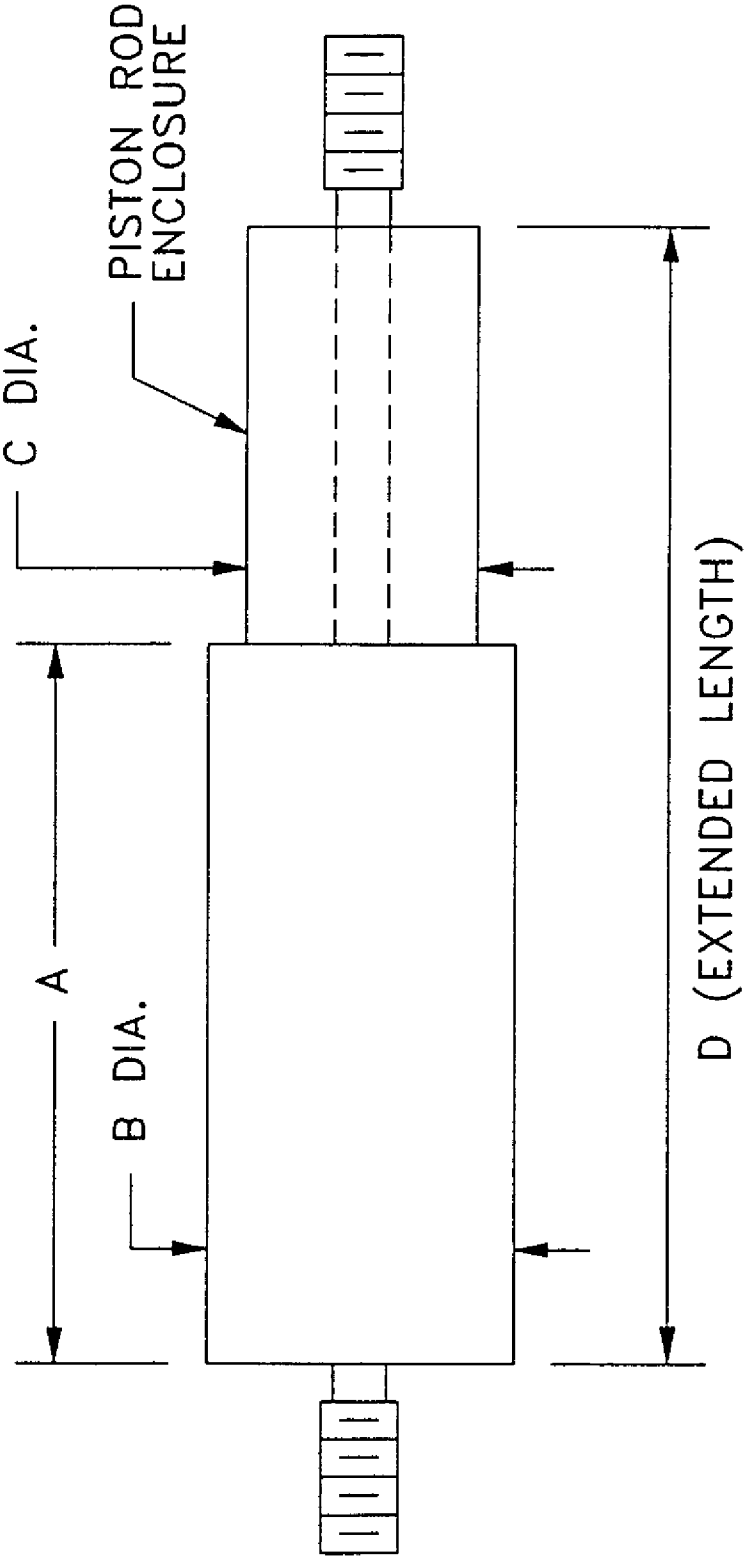

FIGURE 2-4 Geometrical Characteristics of Fluid Viscous Dampers (Refer to Table 2-I)

TABLE 2-I Characteristics of Fluid Viscous Dampers
(1 in. = 25.4 mm, 1 Kip = 4.46 KN, 1 lb = 4.46 N)

MODEL	MAX. FORCE (Kips)	STROKE (in.)	WEIGHT (lbs)	A (in.)	B (in.)	C (in.)	D (in.)
1.5 X 4 *	2	4	2.33	9.0	1.50	w/out enclosure	13.0
3 X 4	10	4	20	11.9	3.00	2.59	17.5
4 X 5	20	5	40	12.7	4.00	3.38	20.5
5 X 5	30	5	50	14.1	5.00	4.38	22.5

Weight is for all steel construction.
* = Tested Damper

may be noted that commercially available dampers are capable of producing significant force output while having small dimensions.

2.4 Mechanical Properties

2.4.1 General Equations

The frequency and amplitude of the motion of the damper piston was specified for each test. The actuator was run under displacement control such that the resulting motion of the damper piston was sinusoidal. The damper motion is given by

$$u = u_0 \sin(\omega t) \tag{2-3}$$

where u_o is the amplitude of the displacement, ω is the frequency of motion, and t is the time. For steady-state conditions, the force needed to maintain this motion is

$$P = P_o \sin(\omega t + \delta) \tag{2-4}$$

where P_o is the amplitude of the force, and δ is the phase angle. The area within the recorded force-displacement loops can be measured to determine the energy dissipated in a single cycle of motion

$$W_d = \oint P\,du = \pi P_o u_o \sin(\delta) \tag{2-5}$$

Rewriting Equation 2-4,

$$P = P_o \sin(\omega t)\cos(\delta) + P_o \cos(\omega t)\sin(\delta) \tag{2-6}$$

and introducing the quantities

$$K_1 = \frac{P_o}{u_o}\cos(\delta) \quad , \quad K_2 = \frac{P_o}{u_o}\sin(\delta) \tag{2-7}$$

where K_1 is the storage stiffness and K_2 is the loss stiffness, one obtains

$$P = K_1 u_o \sin(\omega t) + K_2 u_o \cos(\omega t) \qquad (2\text{-}8)$$

Equation 2-8 may also be written the form

$$P = K_1 u + \frac{K_2}{\omega}\dot{u} \qquad (2\text{-}9)$$

where it is clear that the first term represents the force due to the stiffness of the damper which is in-phase with the motion and the second term represents the force in the damper due to the viscosity of the damper which is 90° out-of-phase with the motion. The damping coefficient is given by

$$C = \frac{K_2}{\omega} \qquad (2\text{-}10)$$

Combining Equations 2-5 and 2-7,

$$K_2 = \frac{W_d}{\pi u_o^2} \qquad (2\text{-}11)$$

$$\delta = \sin^{-1}\left(\frac{K_2 u_o}{P_o}\right) \qquad (2\text{-}12)$$

Equations 2-7 and 2-10 through 2-12 can now be used to obtain the mechanical properties of the damper from experimentally measured values of W_d , P_o , and u_o. First the loss stiffness is determined from Equation 2-11. Knowing the imposed frequency, ω, the damping coefficient is determined from Equation 2-10. Equation 2-12 is used to compute the phase angle. Finally, the storage stiffness is computed using Equation 2-7.

2.4.2 Experimental Results

A total of 58 tests were conducted in the frequency range of 0.1 to 25 Hz, peak velocity range of 0.65 in/sec to 18.2 in/sec (16.5 to 462.3 mm/sec) and at three temperatures: about 0°C, room

temperature (about 22°C), and about 50°C. In all tests, 5 cycles were completed. Table 2-II summarizes the results.

The low temperature tests were conducted with the arrangement of Figure 2-5 in which the damper was encased in a plastic cylindrical tube containing a pack of ice with alcohol to lower the temperature. The high temperature tests were conducted with the arrangement of Figure 2-6 in which the damper was encased in a cardboard cylindrical tube wrapped with teflon tape with a temperature adjustable heating unit wrapped around it several times. The heating unit generated heat which was transferred to the space between the damper and the cylindrical tube. In all cases, a thermocouple monitored the surface temperature of the housing of the device.

Typical recorded force-displacement loops are presented in Figure 2-7 at temperatures of 1°C, 23°C and 47°C and frequencies of 1, 2 and 4 Hz. In this range of frequency of motion, the device exhibits insignificant storage stiffness and its behavior is essentially linear viscous. One should compare the peak force in the tests with frequency of 2 and 4 Hz (amplitude is such that the peak velocity is the same). The recorded peak forces in the two tests are almost identical.

At frequencies above about 4 Hz, the device exhibited storage stiffness which reached values approximately equal to the loss stiffness at frequencies exceeding 20 Hz. Figure 2-8 demonstrates this behavior in a test at frequency of 20 Hz and amplitude of 0.05 in (1.27 mm).

The mechanical properties of the device were almost completely independent of the amplitude of motion. This was confirmed in tests conducted at the same frequency and different amplitude. For example, one should compare the results of tests 32 and 33 and tests 39 and 40 in Table 2-II. Further confirmation of this

TABLE 2-II Summary of Component Tests and Mechanical Properties
(1 in = 25.4 mm, 1 lb = 4.46 N)

TEST	FREQUENCY (Hz)	AMPLITUDE (in)	PEAK VELOCITY (in/sec)	PEAK FORCE (lb)	DISSIPATED ENERGY (lb-in)	STORAGE STIFFNESS (lb/in)	LOSS STIFFNESS (lb/in)	DAMPING COEFFICIENT (lb-sec/in)	PHASE ANGLE (degrees)	TEMPERATURE (°C)
1	0.1	1.03	0.647	71.3	229.1	0	68.7	109.3	90	23
2	0.1	1.03	0.647	71.0	236.2	0	70.9	112.8	90	23
3	0.1	1.03	0.647	80.7	263.5	0	79.1	125.9	90	23
4	0.1	1.03	0.647	85.4	291.6	0	87.5	139.3	90	22
5	0.1	1.03	0.647	85.2	290.8	0	87.3	138.9	90	23
6	0.1	1.03	0.647	59.2	202.4	0	60.7	96.6	90	48
7	0.2	0.51	0.646	106.7	168.4	0	202.9	161.5	90	2
8	0.2	0.51	0.646	69.5	113.8	0	1137.1	109.1	90	23
9	0.2	1.03	1.294	201.9	660.0	0	198.0	157.6	90	2
10	0.2	1.03	1.294	145.2	471.2	0	141.4	112.5	90	23
11	0.4	0.26	0.646	66.5	54.9	0	264.6	105.3	90	23
12	0.4	0.26	0.651	66.5	52.8	0	250.5	99.7	90	23
13	0.4	0.26	0.643	105.0	70.4	0	341.9	136.0	90	2
14	0.6	1.03	3.883	385.9	1240.7	0	372.3	98.8	90	23
15	1.0	0.99	6.220	576.0	1756.7	0	570.5	90.8	90	26
16	1.0	1.02	6.409	624.1	1985.7	0	607.5	96.7	90	23
17	1.0	1.03	6.472	604.1	1990.2	0	597.1	95.0	90	23
18	1.0	1.03	6.472	609.2	1938.7	0	581.7	92.6	90	22
19	1.0	1.03	6.472	848.0	2672.4	0	801.8	127.6	90	2
20	1.0	1.03	6.472	434.6	1399.1	0	419.8	66.8	90	47
21	1.5	1.01	9.519	871.4	2777.8	0	866.8	92.0	90	23